CONVERTING KNOWLEDGE INTO VALUE FOR OVER 30 YEARS

Since 1986

Study of a novel curved single lap joint concept with non-uniform adhesive thickness

Dia Mundial dos Materiais 2023

08/11/2023

V.D.C. Pires[1,2], R.J.C. Carbas [2,3], E.A.S. Marques [3], L.F.M. da Silva [3]

[1] Chair of Designing Plastics and Composite Materials, Department of Polymer Engineering and Science, Montanuniversitaet Leoben, Otto Glöckel-Straße 2, Leoben, 8700, Austria

[2] Institute of Science and Innovation in Mechanical and Industrial Engineering (INEGI), Rua Dr. Roberto Frias, 4200-465 Porto, Portugal

[3] Department of Mechanical Engineering, Faculty of Engineering, University of Porto, Porto, Portugal

CONTENT

inegi driving science & innovation

Advanced Joining Processes Unit

Since 1986

U.PORTO

1.

Introduction

- 1.1. Background and motivation
- 1.2. The curved joint concept

inegi driving science & innovation

Advanced Joining Processes Unit

Since 1986

U.PORTO

1.1. Background and motivation

Composite materials in the aeronautical industry

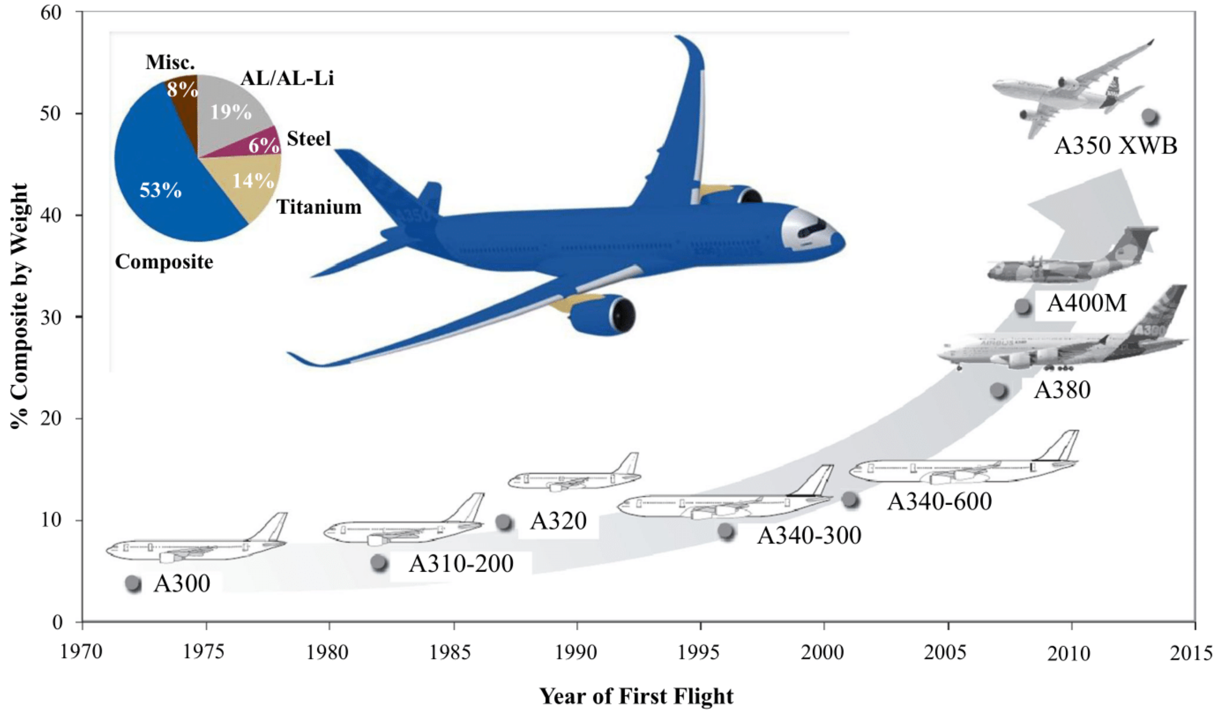

Figure 1 – Trends in the use of composite materials in commercial aircrafts [Xu et al., 2018].

1.1. Background and motivation

Regulatory hurdles regarding adhesive bounding

Non-destructive testing limitations and **delamination** caused are key barriers to the widespread adoption of adhesive bonding in aircraft structures.

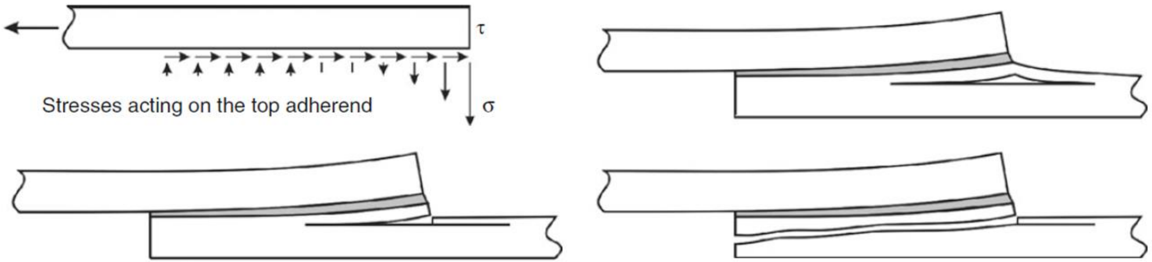

Figure 2 – Peel stress failure in adhesively bonded composite adherends [Hart Smith, 1973].

(a)

(b)

Figure 3 – Most prominent aviation regulatory bodies. (a) EASA in EU. (b) FAA in the US.

1.2. The curved joint concept

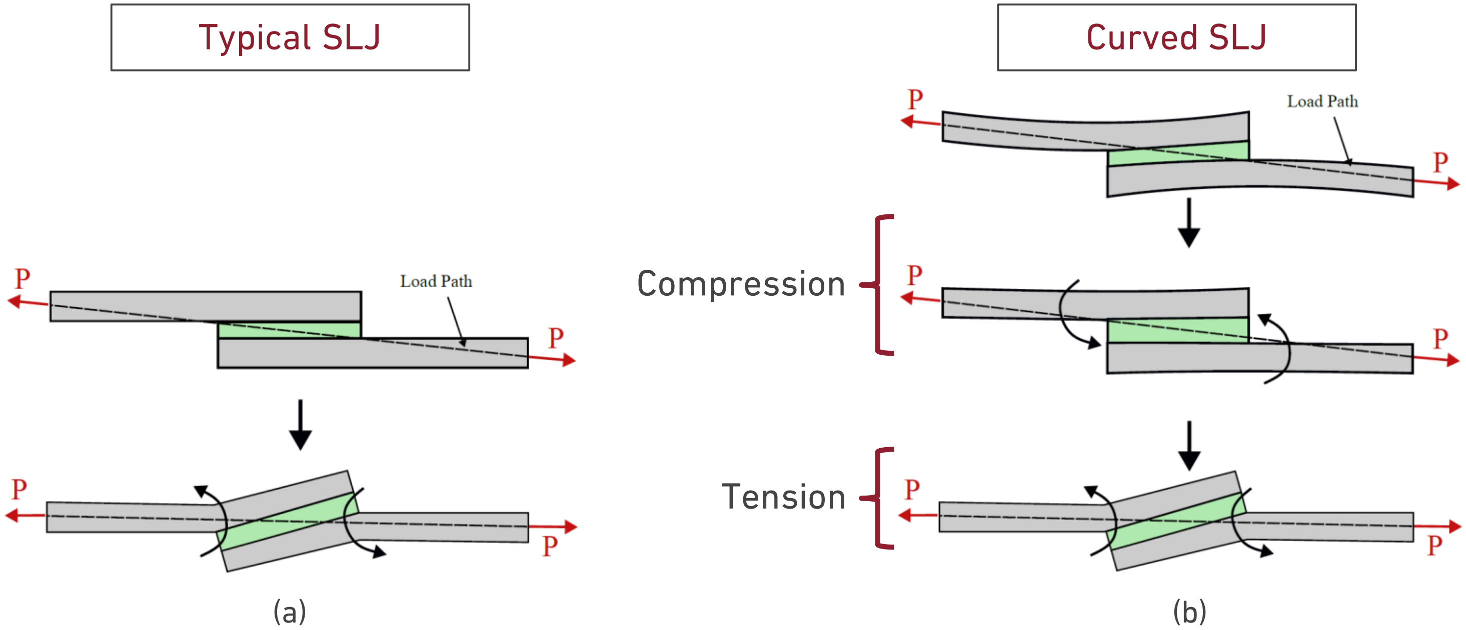

Figure 4 – Behaviour of SLJ under traction. (a) Planar SLJ. (b) Curved SLJ..

2.

Experimental procedures

- 2.1. SLJ manufacturing
- 2.2. SLJ testing

driving science & innovation

Advanced Joining Processes Unit

Since 1986

U.PORTO

2.1. SLJ manufacturing

SLJ configurations and geometry

Metal SLJ

Reference 0.2 mm

Curved

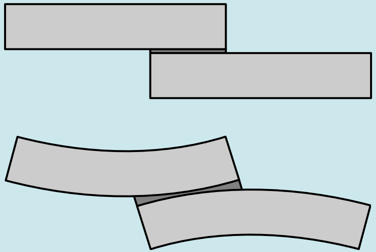

Composite SLJ

Reference 0.2 mm

Reference 1.0 mm

Curved

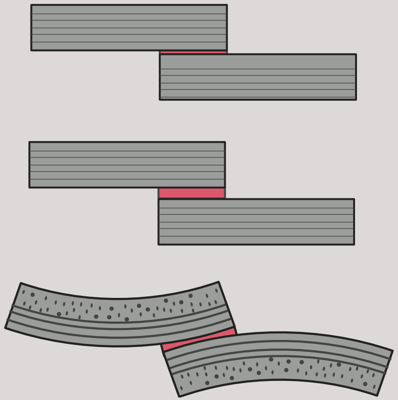

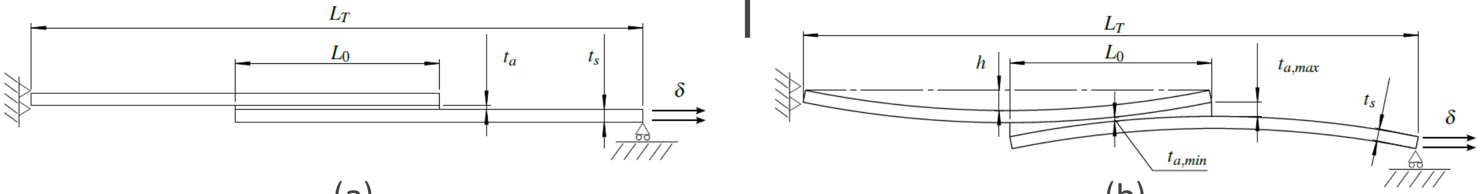

(a) (b)

Figure 5 – SLJ specimen geometry. (a) Planar SLJ. (b) Curved SLJ.

2.2. SLJ testing

All tests were performed in an Instron® 3832 (Norwood, MA, USA) **quasi-static machine**.

Testing speed: 1mm/min

Standards followed:

1. ASTM D5868 (Composite SLJ)
2. ASTM D1002 (Metal SLJ)

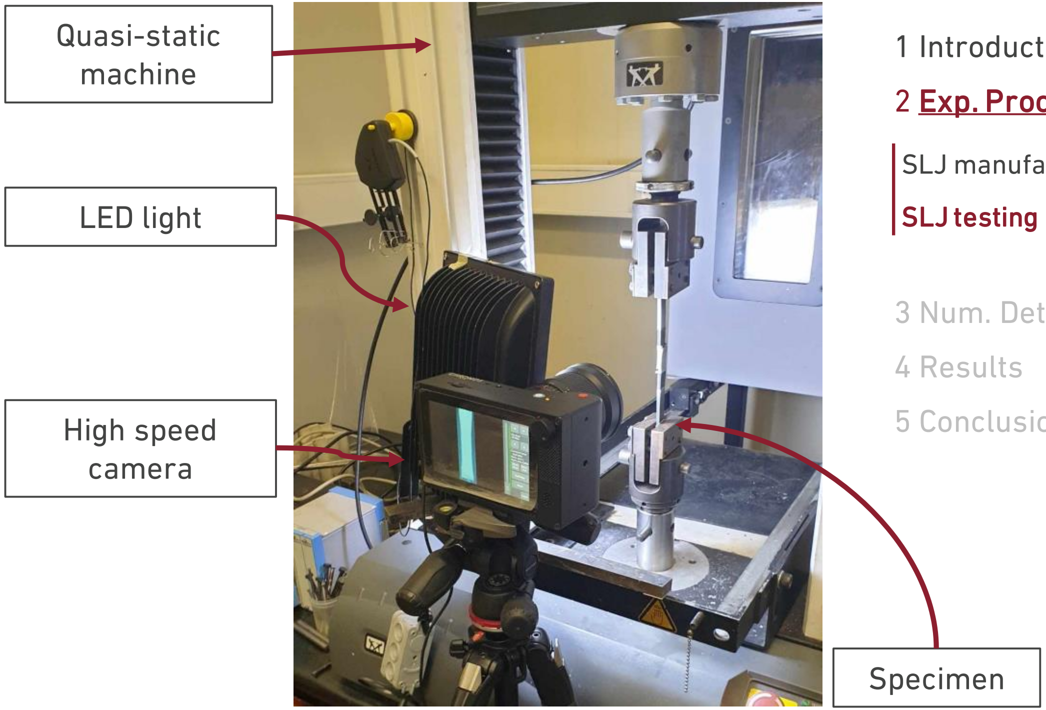

Figure 6 – Experimental setup.

3.

Numerical details

- 3.1. Metal SLJ
- 3.2. Composite SLJ

Since 1986

3.1. Metal SLJ

Parametric elasto-plastic models

Nomenclature: $\Delta t_a\ X$, refers to the model with Xmm of extra maximum thickness relative to the reference

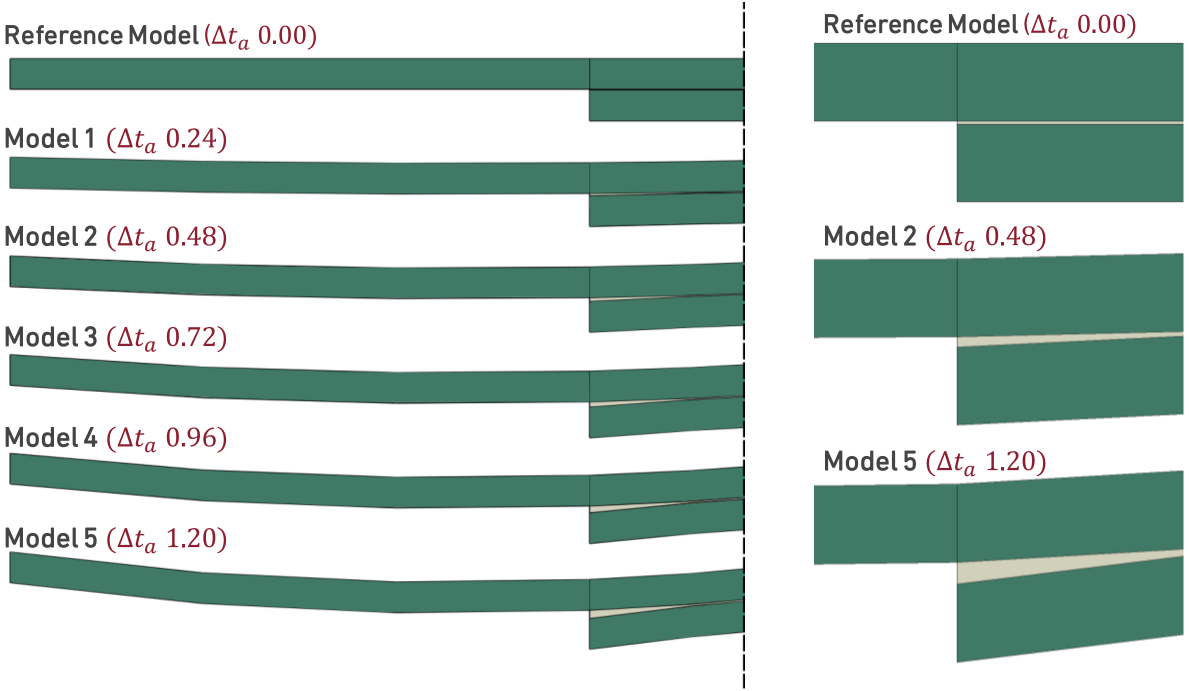

Fig.7 – Parametric study with varying curvatures and maximum adhesive thicknesses. 2D static analysis in ABAQUS® software CPE4R elements (Plane Strain) were used for the elastic model

3.1. Metal SLJ

CZM Models

Aluminium (Elasto-plastic)

Adhesive (Elastic)

Adhesive (Cohesive)

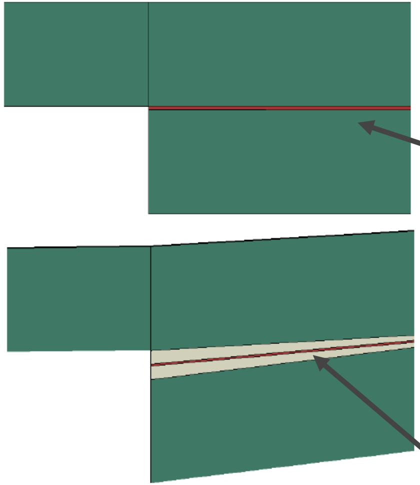

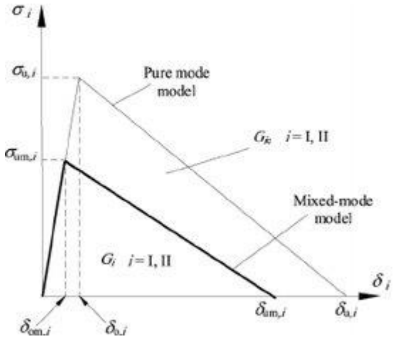

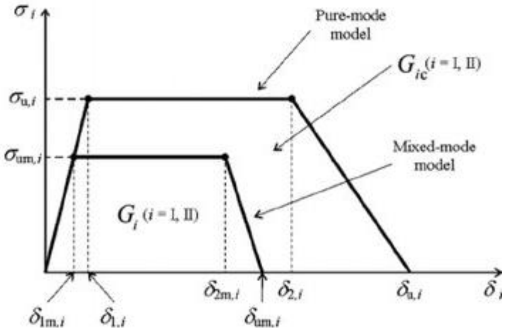

- 2D static analysis in ABAQUS® software
- **CPE4 elements** (Plane Strain) for the elastic sections
- **COH2D4 elements** (Cohesive) for the cohesive section

3.2. Composite SLJ

CZM and XFEM models

CFRP (Elastic)

CFRP (Cohesive)

Adhesive (Elastic)

Adhesive (Cohesive)

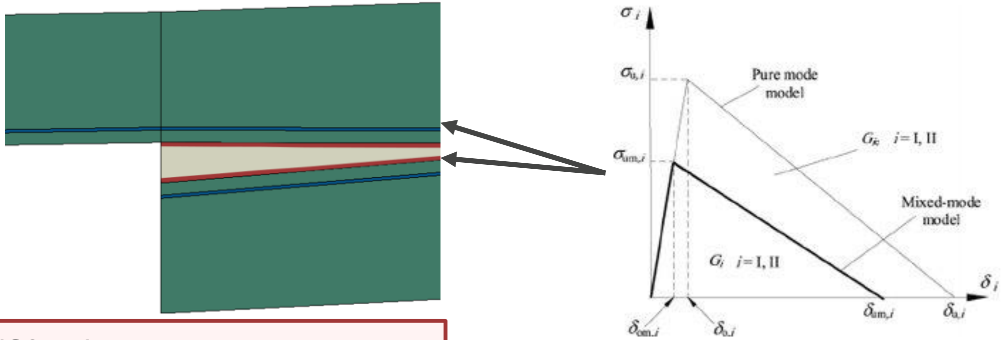

- 2D static analysis in ABAQUS® software
- **CPE4 elements** (Plane Strain) for the elastic sections
- **COH2D4 elements** (Cohesive) for the cohesive section

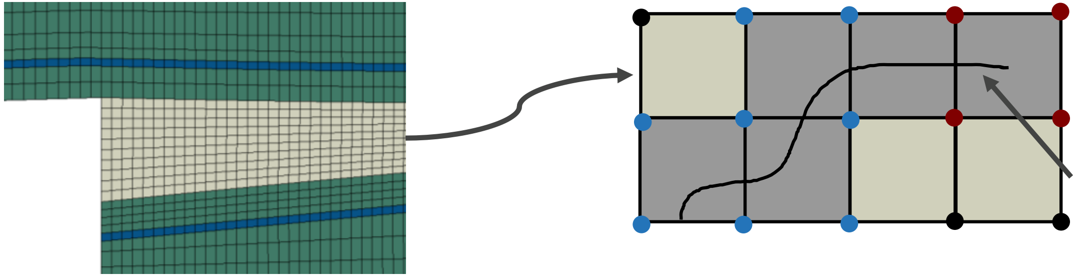

XFEM crack domain

Enriched elements

Crack surface

4.

Results

- 4.1. Metal SLJ
- 4.2. Composite SLJ

Since 1986

4.1. Metal SLJ

Stress distributions

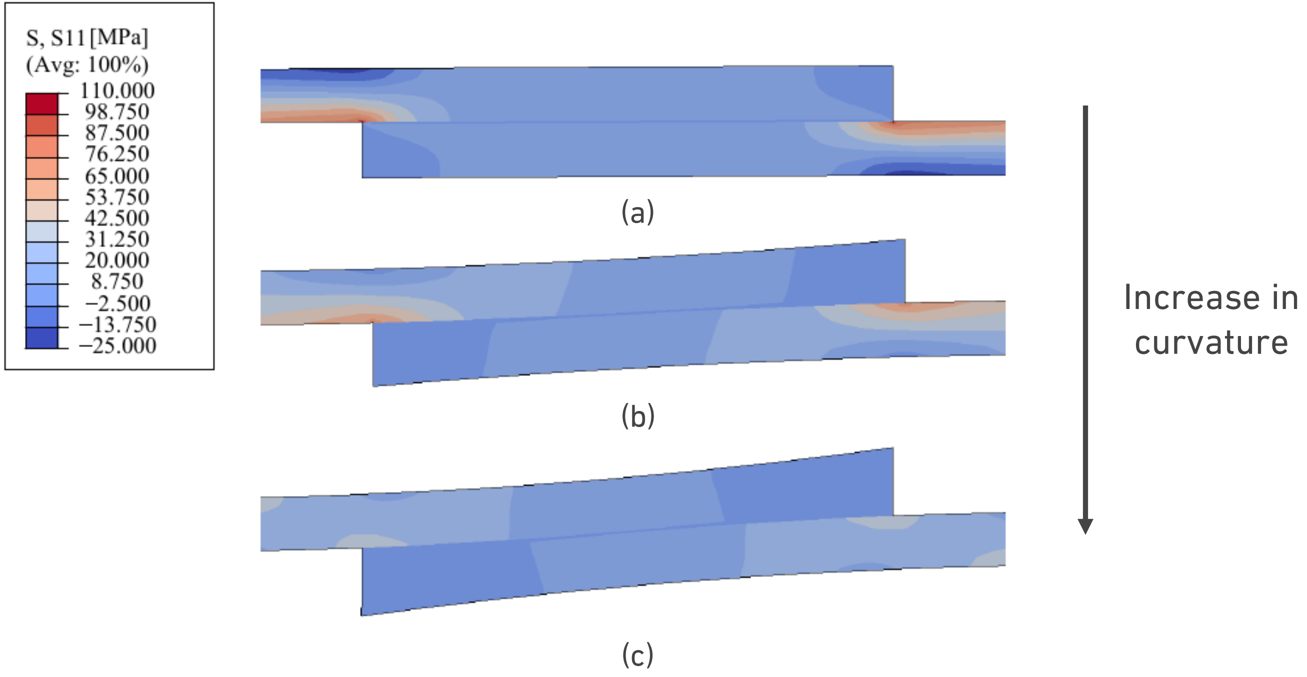

Fig.8 – Longitudinal stresses in MPa along the overlap length for the elastic models. (a) Reference. (b) Model 3. (c) Model 5.

4.1. Metal SLJ

Peel stress distributions

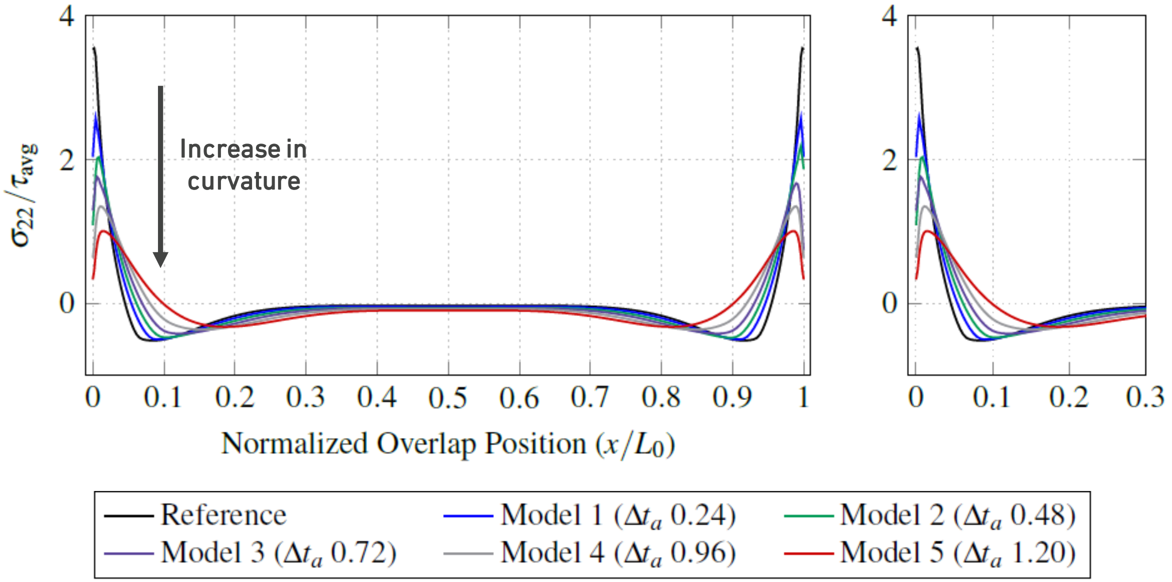

Fig.9 – Normalized peel stress distributions at the adhesive layer mid-thickness along the overlap.

4.1. Metal SLJ

Joint performance

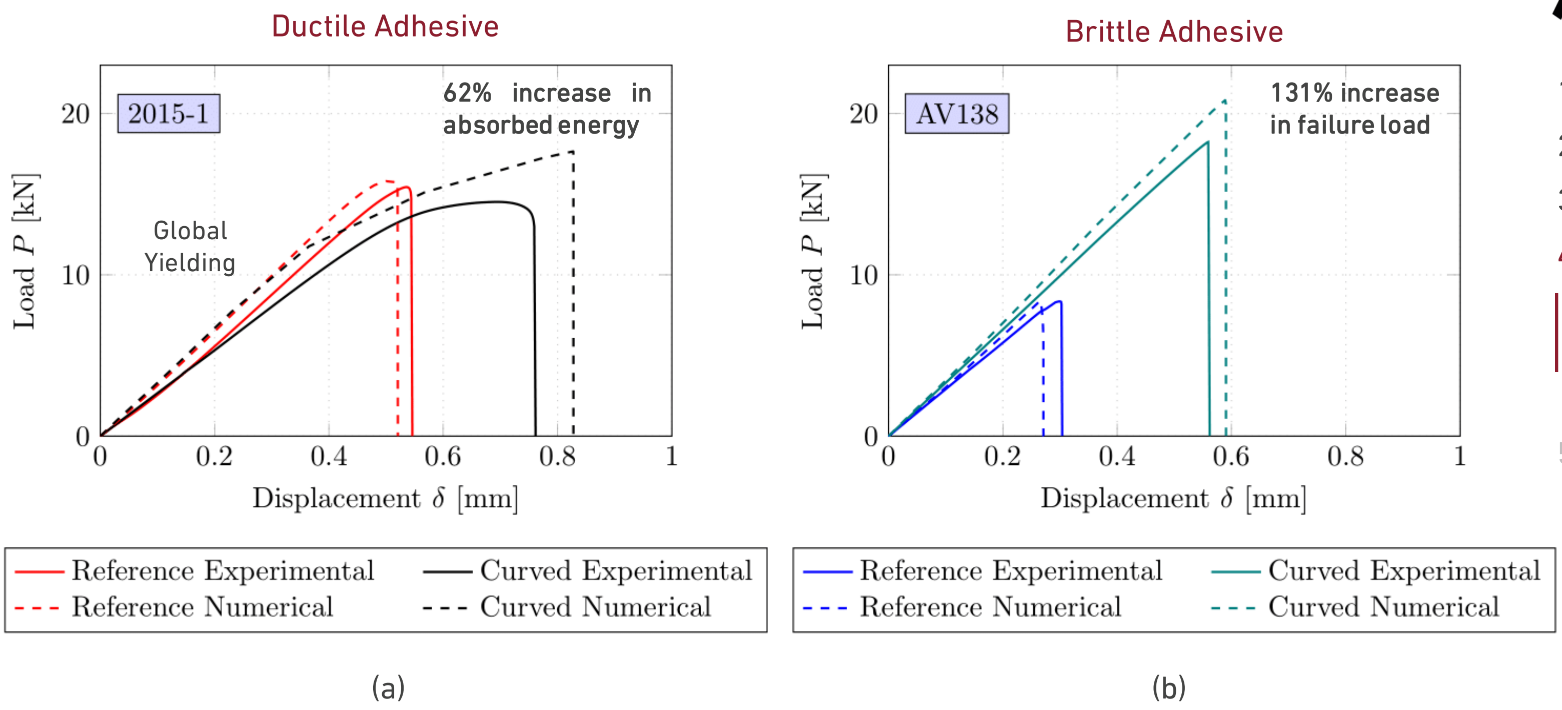

Fig.10 – $P - \delta$ curves obtained experimentally and numerical for both adhesives. The curved configuration corresponds to the geometry with the highest curvature. (a) 2015-1 (b) AV138.

4.2. Composite SLJ

Failure mode

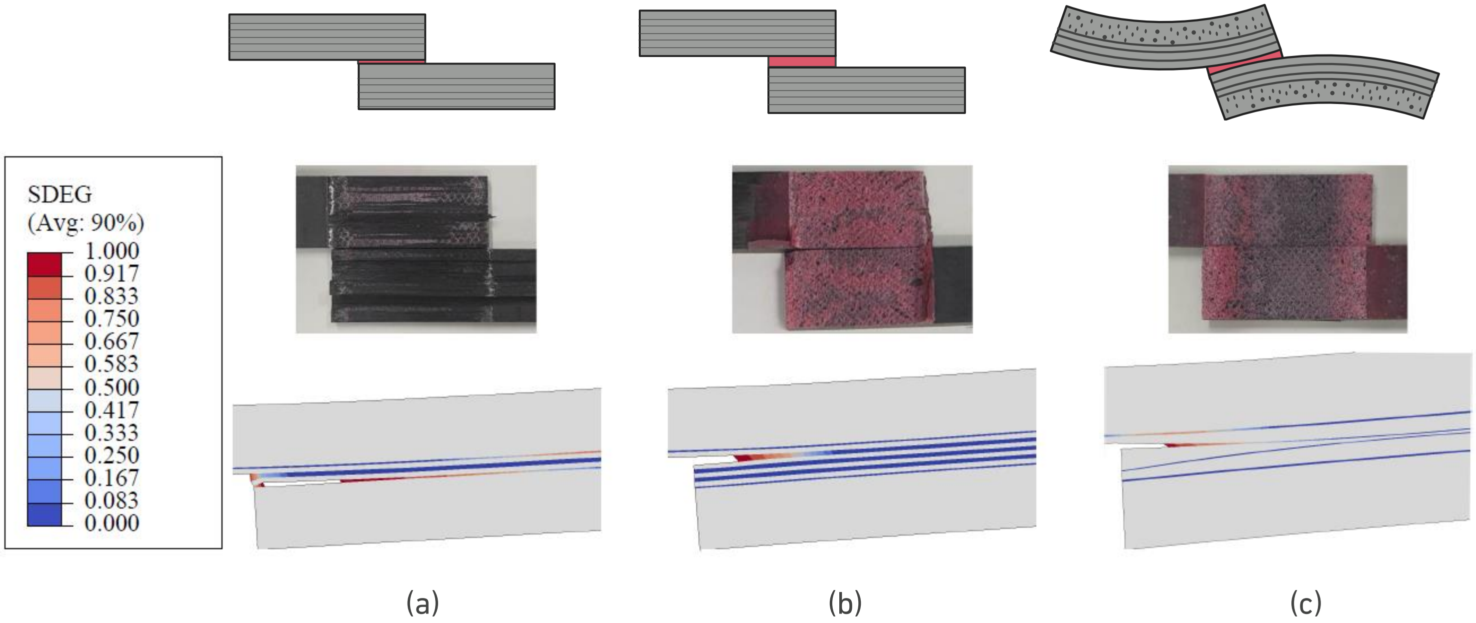

Fig.11 – Experimental and numerical failure mode for the studied SLJ.
(a) Reference 0.2. (b) Reference 1.0mm. (c) Curved.

4.2. Composite SLJ

Joint performance in quasi-static

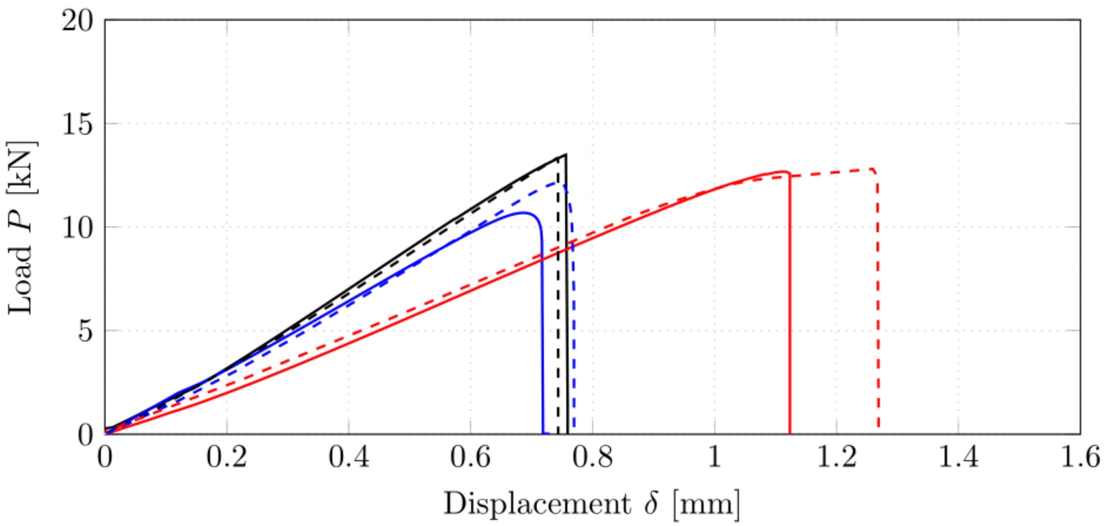

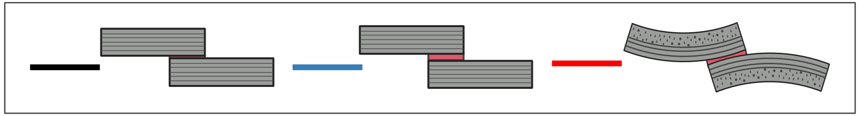

Experimental — — Numerical

Fig.12 – $P - \delta$ curves obtained experimentally and numerical for all configurations.

4.2. Composite SLJ

Crack propagation

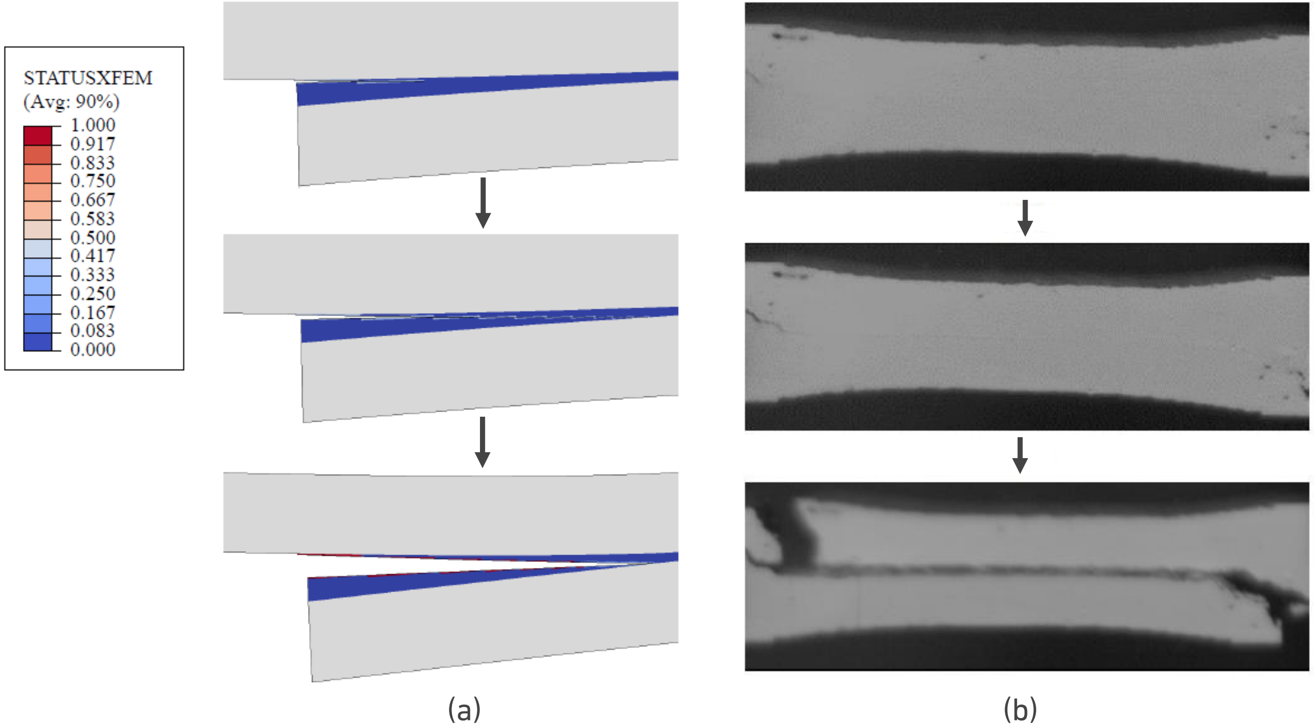

Fig.13 – Crack propagation. (a) Numerical crack prediction. (b) Experimental crack propagation.

4.2. Composite SLJ

Crack propagation

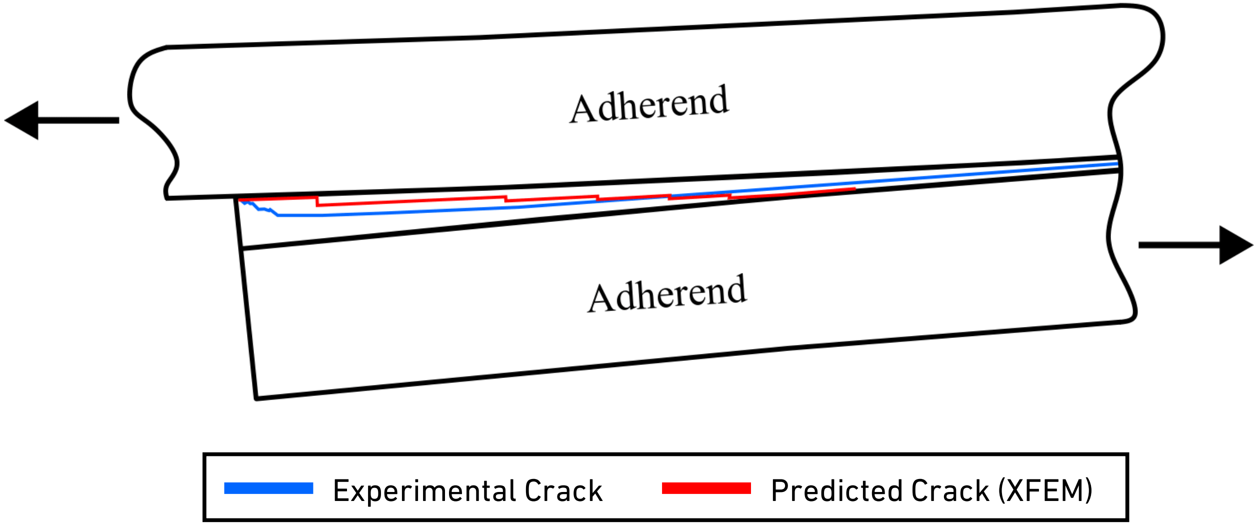

Fig.14 – Comparison between the numerical and experimental cracks.

5.

Conclusions

- 5.1. Conclusions
- 5.2. Scientific output

U.PORTO

inegi driving science & innovation

Advanced Joining Processes Unit

Since 1986

5.1. Conclusions

- This study showed that the use of the curved geometry significantly **decrease** the **peak stresses** in the overlap edges.
- Curved metal SLJs showed **increased energy absorption** with a ductile adhesive and significantly **improved failure load** when using with a brittle adhesive.
- The decrease of peak stresses, namely peel stresses on the overlap edges **prevented delamination**, allowing for a **cohesive** failure modes and improve performance on the composite SLJs in static and higher strain rates scenarios.
- The study demonstrated the promising characteristics of curved substrate SLJs for both metal and composite applications, offering superior failure modes and performance. Further optimization and modifications of the curved configuration are suggested for enhanced performance.

5.2. Scientific output

SLJ Designer for ABAQUS CAE

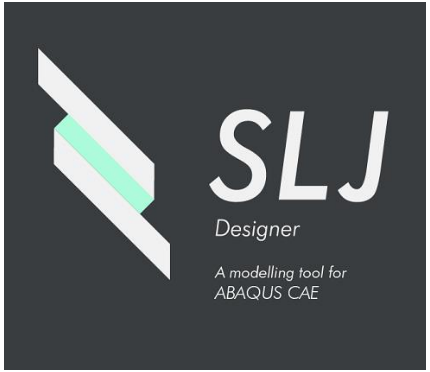

- Generation of SLJ within a costume GUI in ABAQUS CAE;
- Includes linear Elastic, Elasto-Plastic, and CZM models;
- Used by students from the Master's in Mechanical Engineering from FEUP.

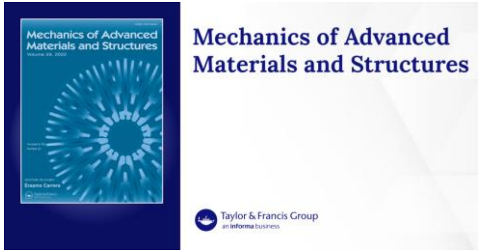

Paper I (Submitted)

Curved Single Lap Joint Design: A Novel Approach to Mitigate Stress Concentrations in Adhesive Joints

<u>V.D.C.Pires</u>, F.C.C.Ribeiro, R.C.J.Carbas, E.A.S.Marques, L.F.M. da Silva

JCM – Sage Journals

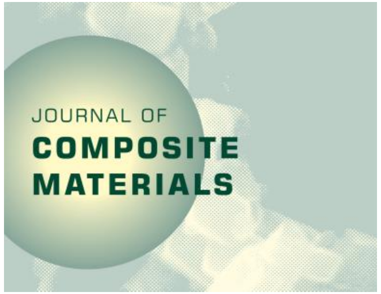

Paper II (Submitted)

Curved Single Lap Joints: An Innovative Approach to Prevent Delamination in CFRP SLJ

<u>V.D.C.Pires</u>, R.C.J.Carbas, E.A.S.Marques, L.F.M. da Silva

5.2. Scientific output - Conferences

☐ Enhancing Joint Performance with Residual Stresses: An Optimization Study on Adhesively Bonded Joints using Dissimilar Joints

V.D.C.Pires, R.C.J.Carbas, E.A.S.Marques, L.F.M. da Silva

Total of 3 presentations and 4 posters in cofnerences

△ Influence of strain-rate in single-lap joints bonding different adherends with thermal residual stresses

☐ Influence of bent adherends in single-lap joint performance

☐ Optimization of dissimilar single-lap joints bonding multimaterial adherends in quasi-static conditions with thermal residual stresses

V.D.C.Pires, R.C.J.Carbas, E.A.S.Marques, L.F.M. da Silva

IAMaC2023
2nd Ibero-American Conference on Composite Materials
20th and 21th of July, 2023

△ The study of residual thermal stresses on the performance of hybrid composite single lap join

V.D.C.Pires, R.C.J.Carbas, E.A.S.Marques, L.F.M. da Silva

△ The influence of bent adherends on adhesively joints strength performance

R.C.J.Carbas, V.D.C.Pires, E.A.S.Marques, L.F.M. da Silva

△ Presentation
☐ Poster

CONVERTING
KNOWLEDGE
INTO VALUE
FOR OVER 30 YEARS

Since 1986

Vasco D.C Pires

vasco.castro-pires@unileoben.ac.at

INSTITUTE OF SCIENCE AND INNOVATION IN MECHANICAL
AND INDUSTRIAL ENGINEERING

www.inegi.up.pt

6.

Backup Slides

SLJ Designer app

Since 1986

SLJ Designer application

ABAQUS python productivity

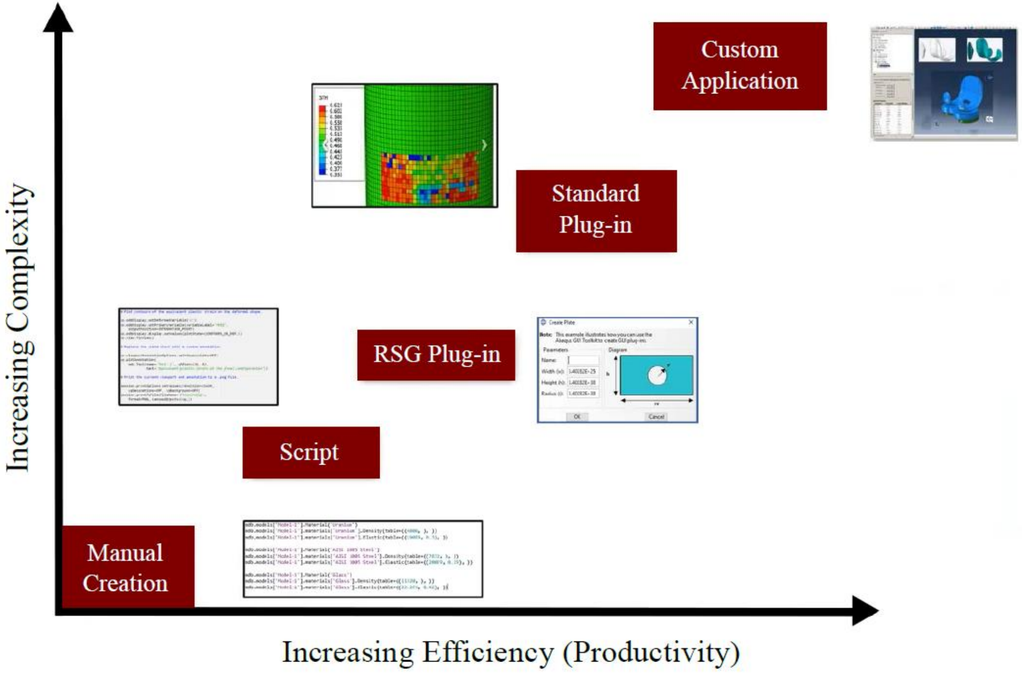

Fig.15 – Automation approaches in ABAQUS ranked by complexity and productivity of the user using Python scripting [Chakraborty, 2021].

SLJ Designer application

Features

ABAQUS CAE classical GUI

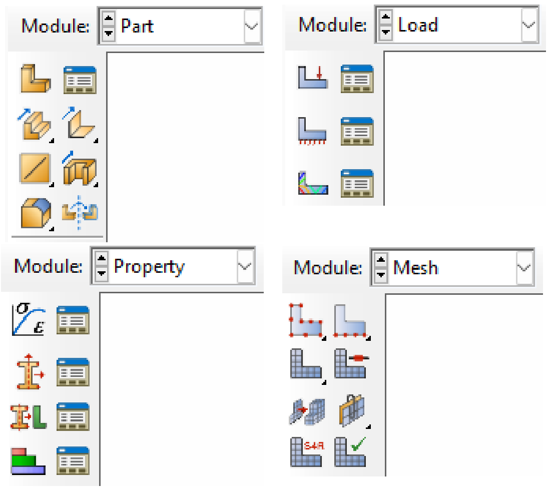

Average time to build a SLJ model:

- Beginner: 1h +
- Advanced: 5-20 mins

SLJ Designer

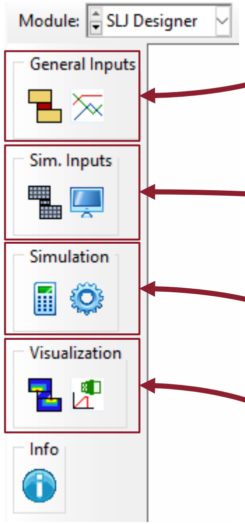

Geometry and Materials (already included in a database)

Simulation details
- Mesh
- B.C
- Thermal step

Model generation and job submission

Visualization and post-processing

Average time to build a SLJ model:

- 1-5 mins (+ 91.6% productivity)

SLJ Designer application

Results utput

SLJ Designer

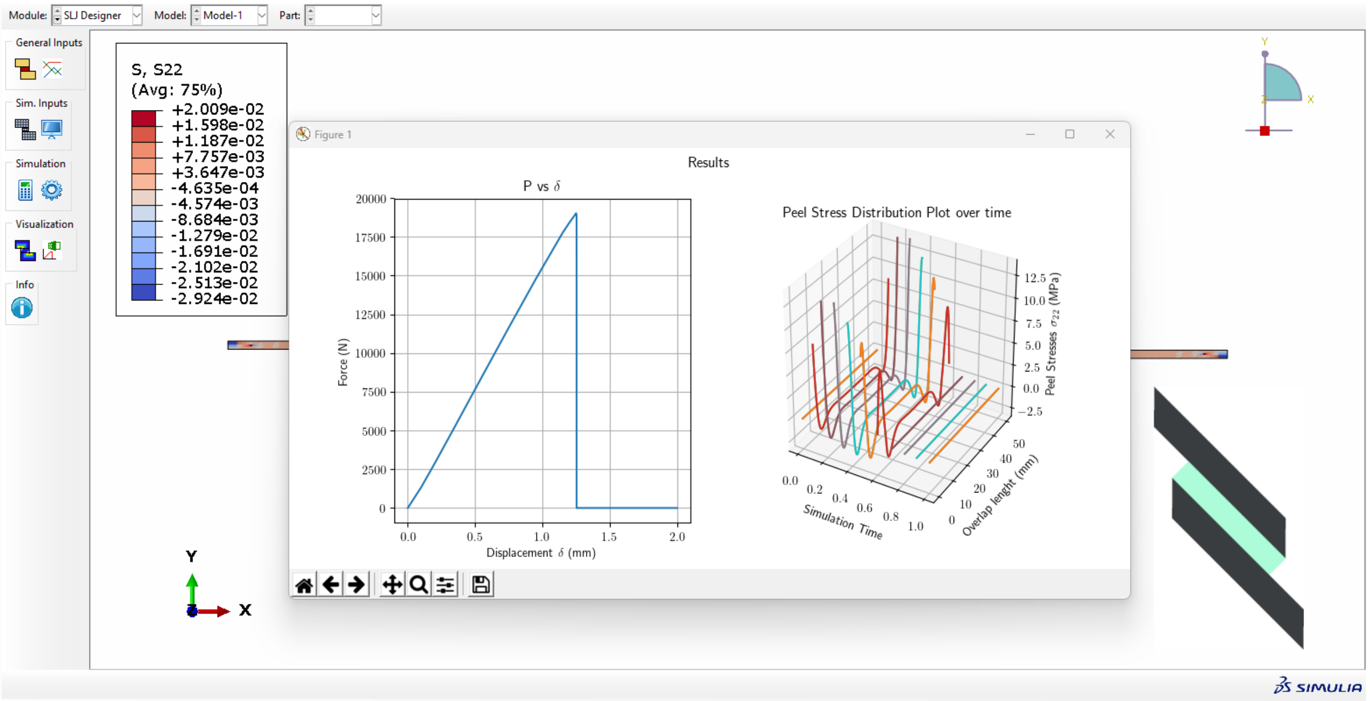

Fig.16 – Post-processing features of SLJ Designer.

SLJ Designer application

Application flowchart

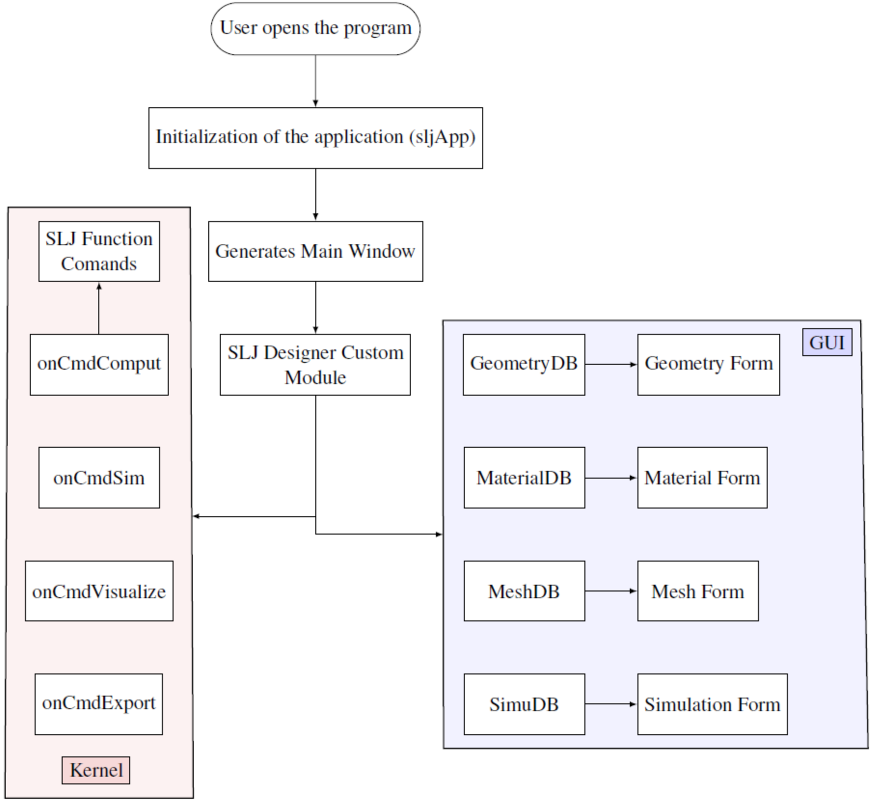

Fig.17 – Automation approaches in ABAQUS ranked by complexity and productivity of the user using Python scripting [Chakraborty, 2021].

SLJ Designer application

Forms GUI

Geometry

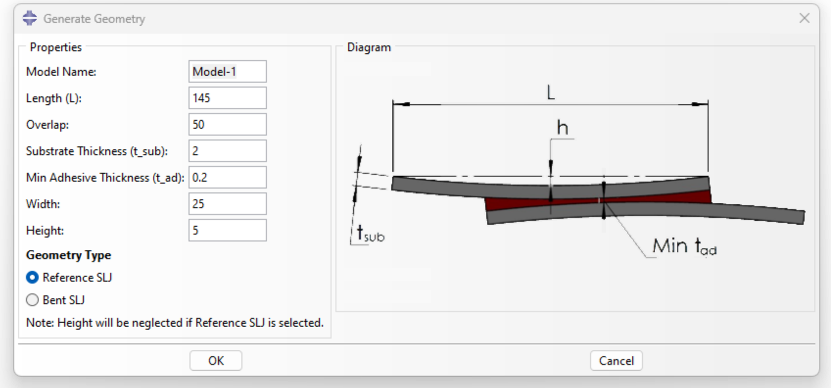

Material Selection

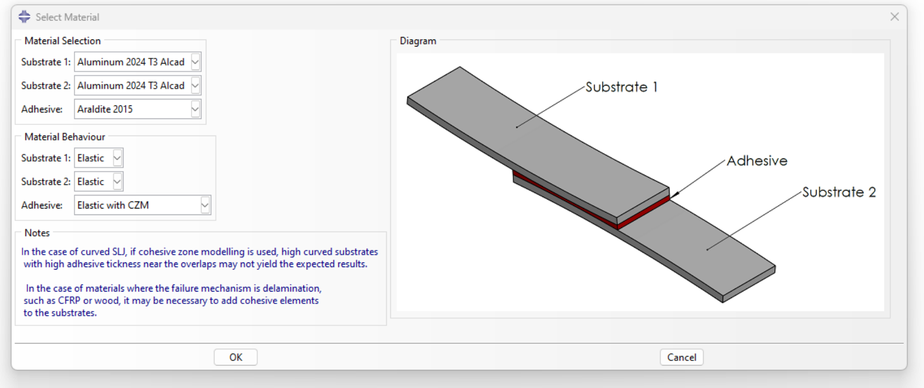

Mesh

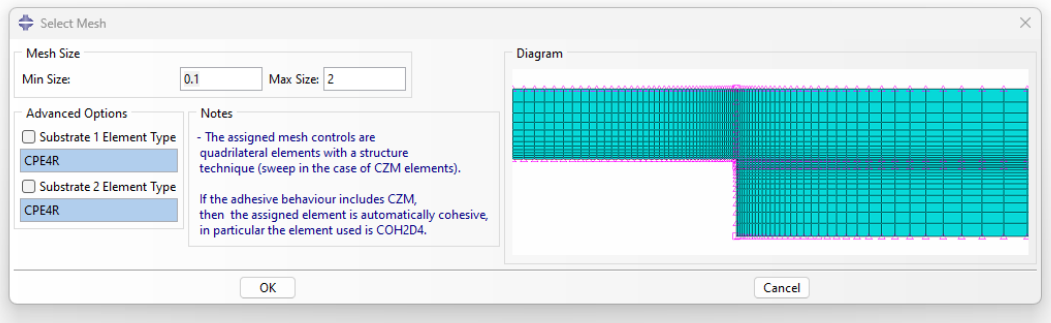

Fig.18 – Some of the forms used in the SLJ application.

SLJ Designer application

Demo Part 1 – Model Generation

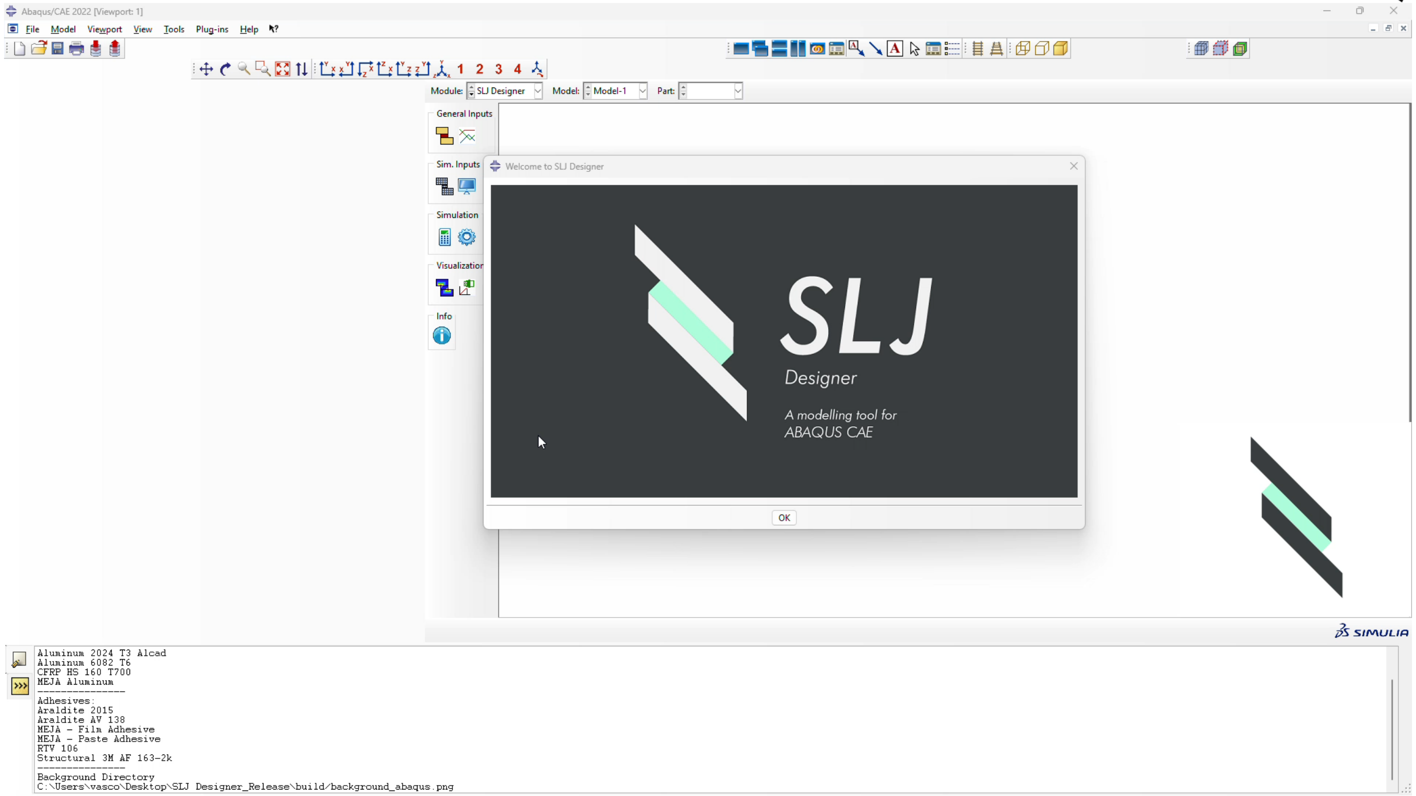

SLJ Designer application

Demo Part 2 – Post Processing

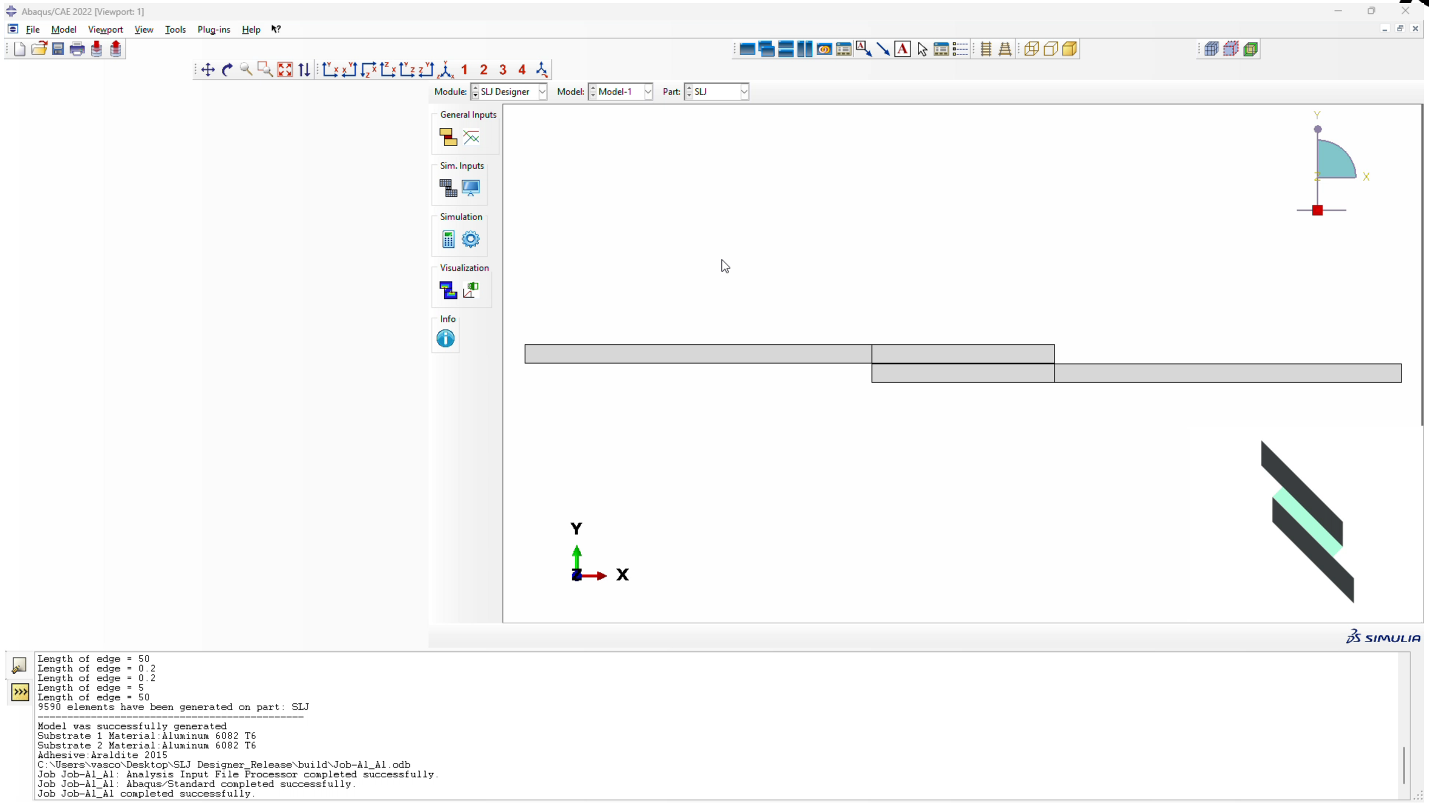

SLJ Designer application

Demo Part 3 – Curved SLJ

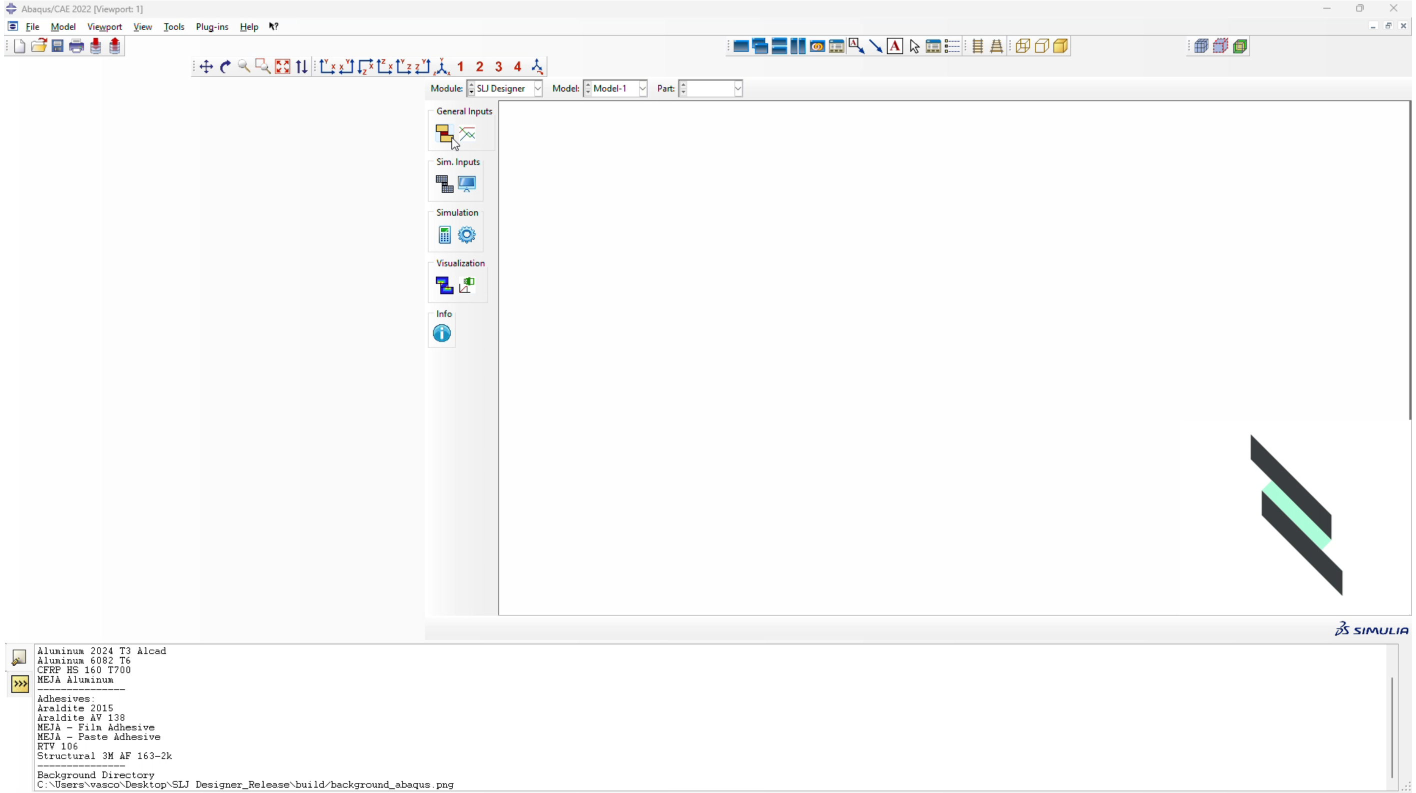

7.

Backup Slides

Experimental details

Since 1986

SLJ manufacturing

Metal SLJ

Adherend curvature was obtained through mechanical **bending** and **plastic deformation**.

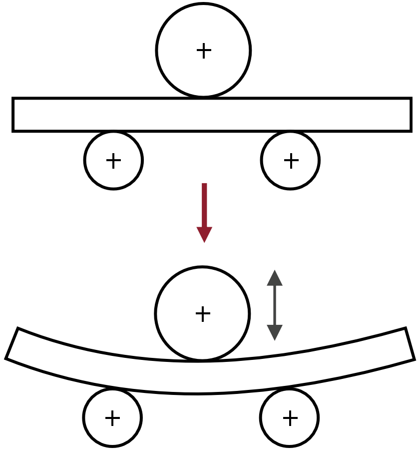

Composite SLJ

Adherend curvature was obtained through **curing** of **asymmetric** composite layup.

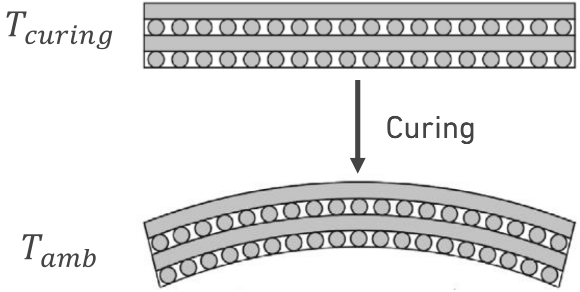

Materials

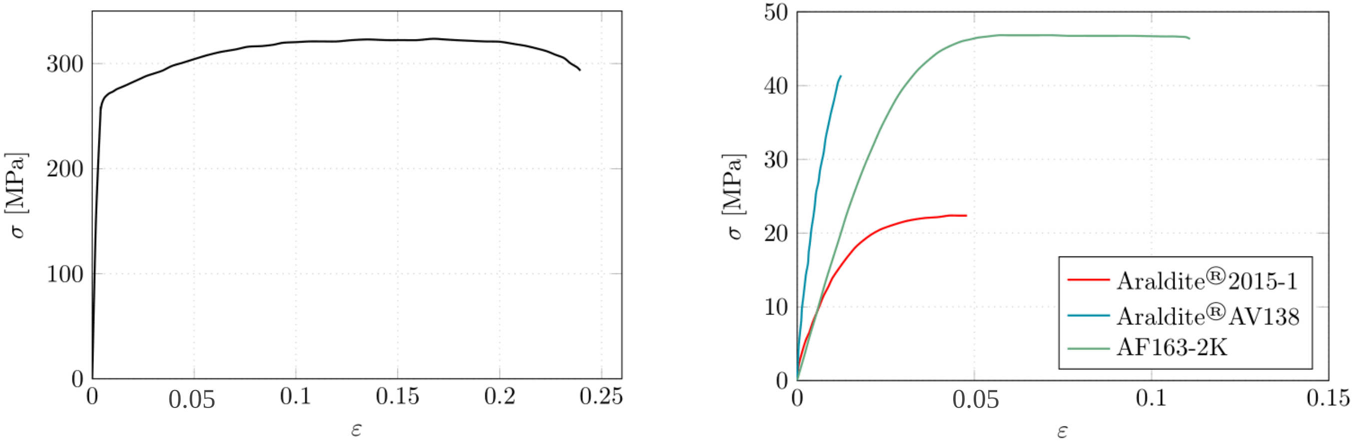

(a) (b)

Figure 19 – Stress-strain curves. (a) Aluminum. (b) Araldite® AV138, Araldite® 2015 and AF163-2K.

Material	E [GPa]	σ_y [MPa]	ν [-]	α [µm/mK⁻¹]
AW6082 T6	67	260	0.3	23.6

Material	E_{11} [GPa]	E_{22} [GPa]	G_{12} [GPa]	ν_{12} [-]	α_{11} [µm/mK⁻¹]	α_{22} [µm/mK⁻¹]
CFRP	109	8819	4.315	0.342	-0.1	26

Adhesive material properties

Table 2 – Properties of the adhesives AV138, 2015-1 and AF 163-2 K.

Property	AV138	2015-1	AF163-2K
Young's modulus, E [MPa]	4890	1850	1520
Poisson's ratio, v [-]	0.35	0.33	0.34
Shear modulus, G [MPa]	1560	560	565
Tensile failure strength, t_n^0 [MPa]	39.5	21.6	46.9
Shear failure strength, t_s^0 [MPa]	30.2	17.9	46.9
Toughness in tension, G_{IC} [MPa]	0.20	0.43	4.05
Toughness in shear,G_{IIC}[MPa]	0.38	4.70	9.77
CTE, α [μm/mK^{-1}]	67	120	90

Metal SLJ manufacturing

Manufacturing process flowchart

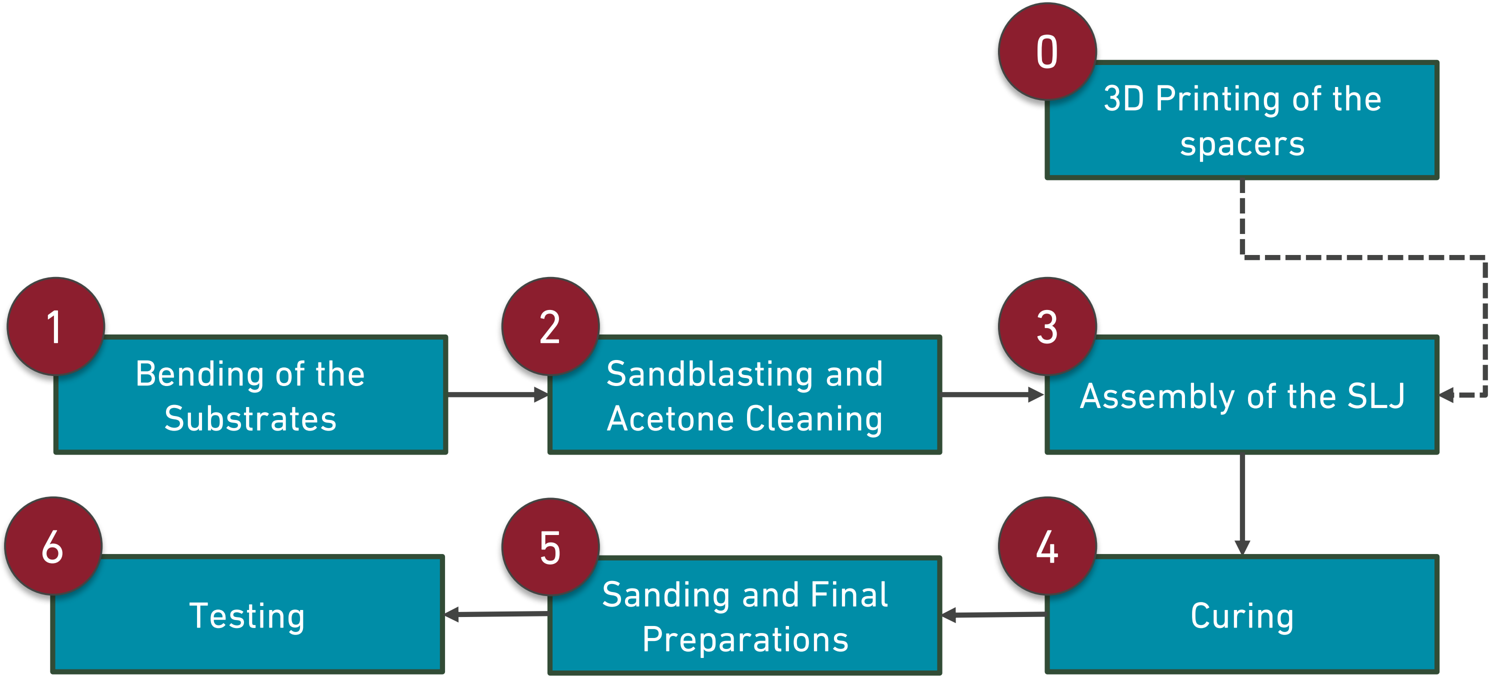

Metal SLJ manufacturing

Manufacturing details

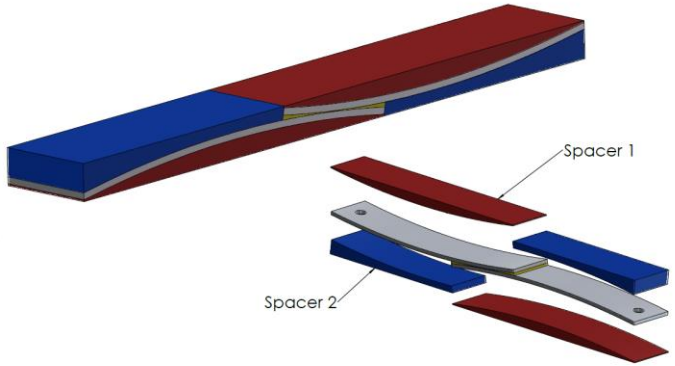

(a)

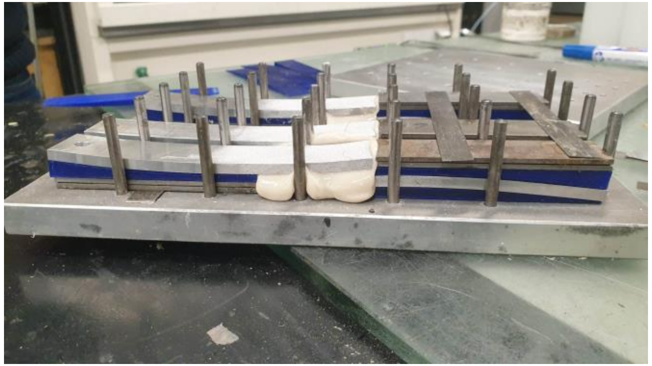

(b)

Figure 20 – (a) CAD of the SLJ. (b) Final assembly of the SLJs before curing.

Name	Type	Curing Conditions
2015-1	Ductile	8h @ T_{Room}
AV138	Brittle	24h @ T_{Room}

CFRP SLJ manufacturing

Manufacturing process flowchart

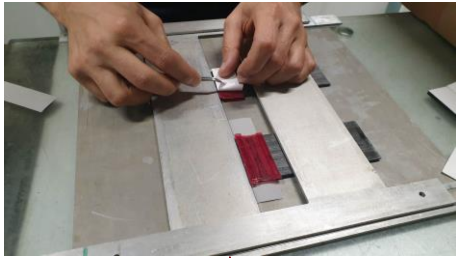

1 Hand layup of the CFRP prepreg plies → 2 Adhesive stacking → 3 Assembly in the mould → 4 Co-Curing → 5 Cutting Specimens

CFRP SLJ manufacturing

Co-curing mechanism (1 step)

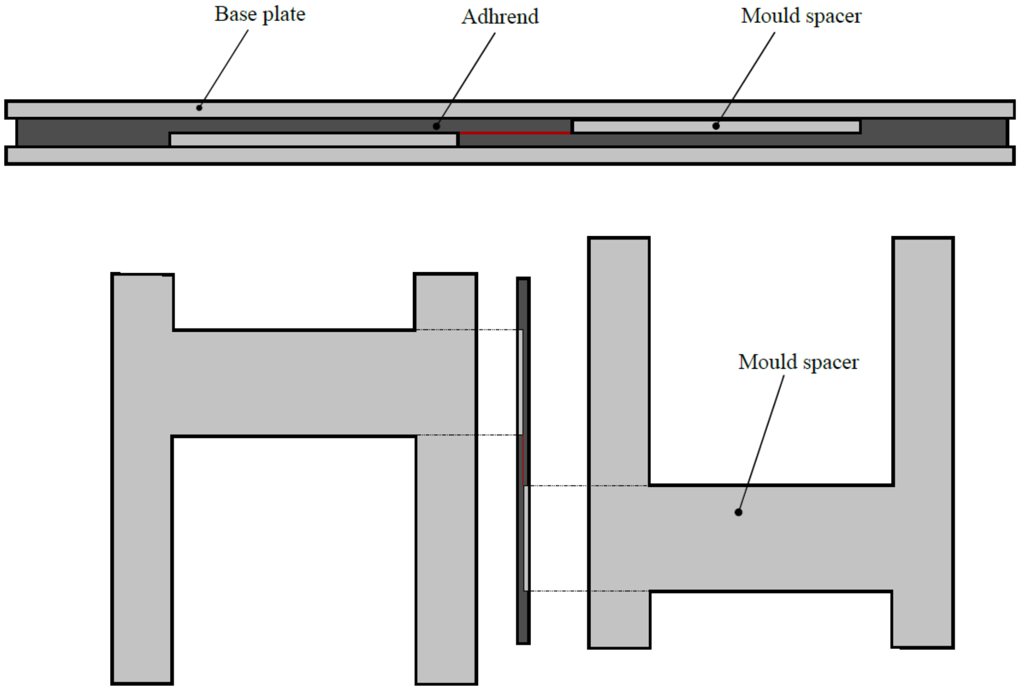

Fig.21 – Manufacturing mould scheme for co-curing.

CFRP SLJ manufacturing

Co-curing mechanism (1 step)

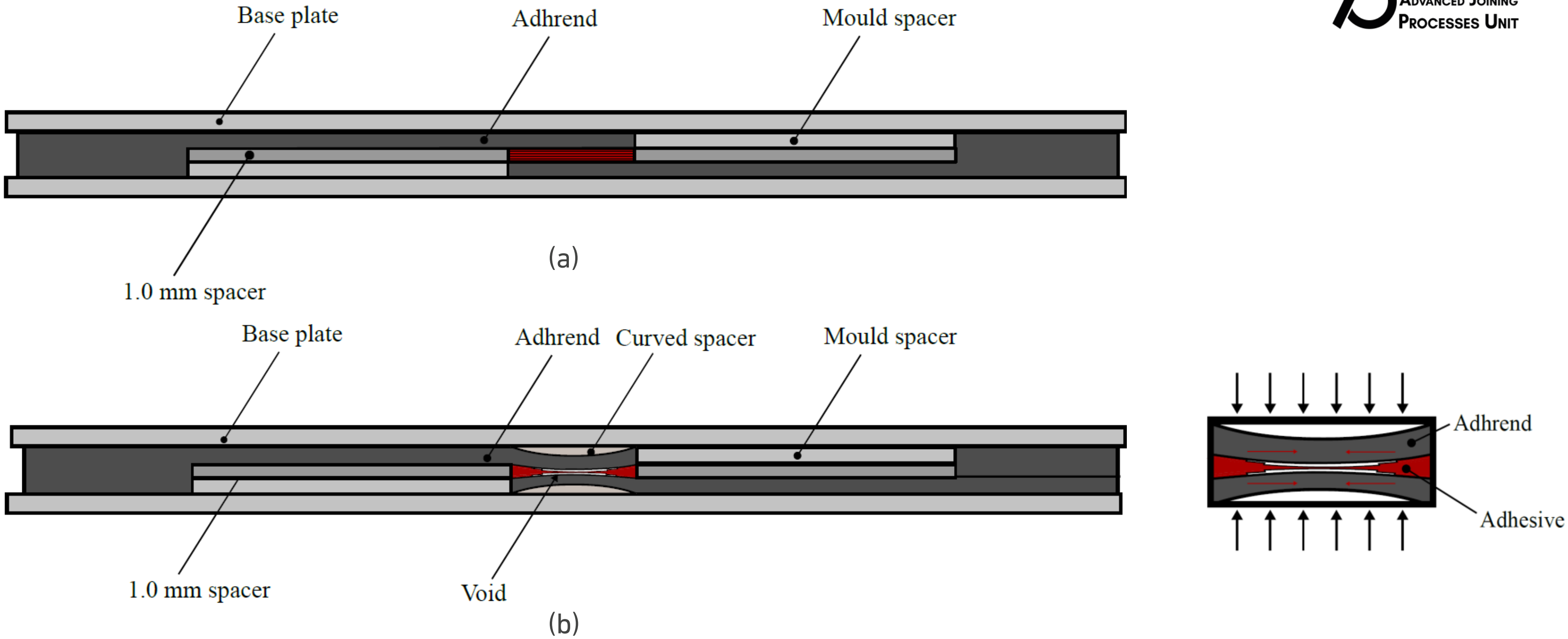

Fig.22 – Manufacturing mould scheme for co-curing of the (a) reference 1.0mm and (b) curved SLJs.

Surface treatments performed

Sandblasting

Phosphoric acid anodization (PAA)

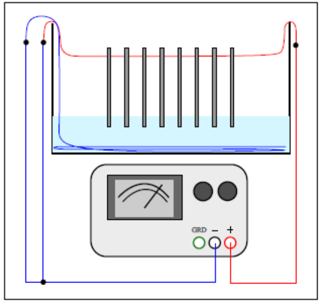

Atmospheric plasma treatment (APT)

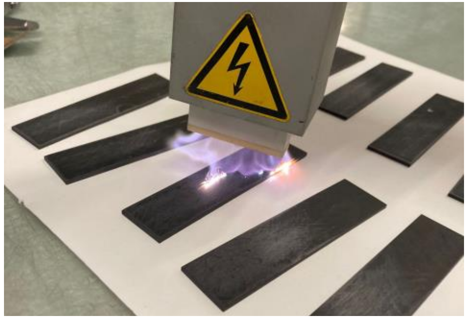

Warpage measurement of composite plates

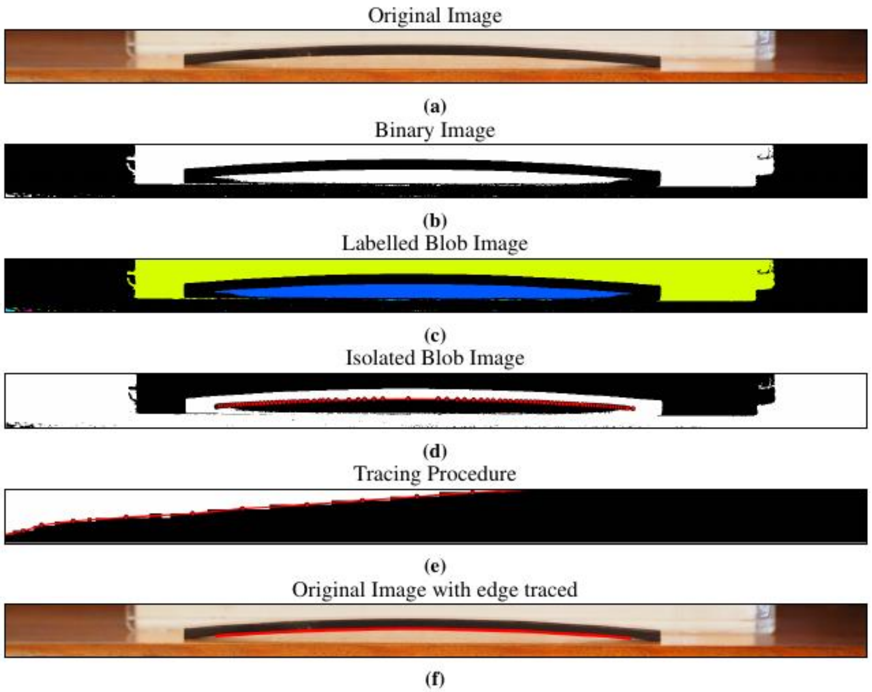

Fig.23 – (a) Original image. (b)-(d) Image processing procedure. (f) Final result where the edge is correctly traced.

8.

Backup Slides

Numerical details and results

U.PORTO

driving science & innovation

Advanced Joining Processes Unit

Since 1986

Mesh and boundary conditions

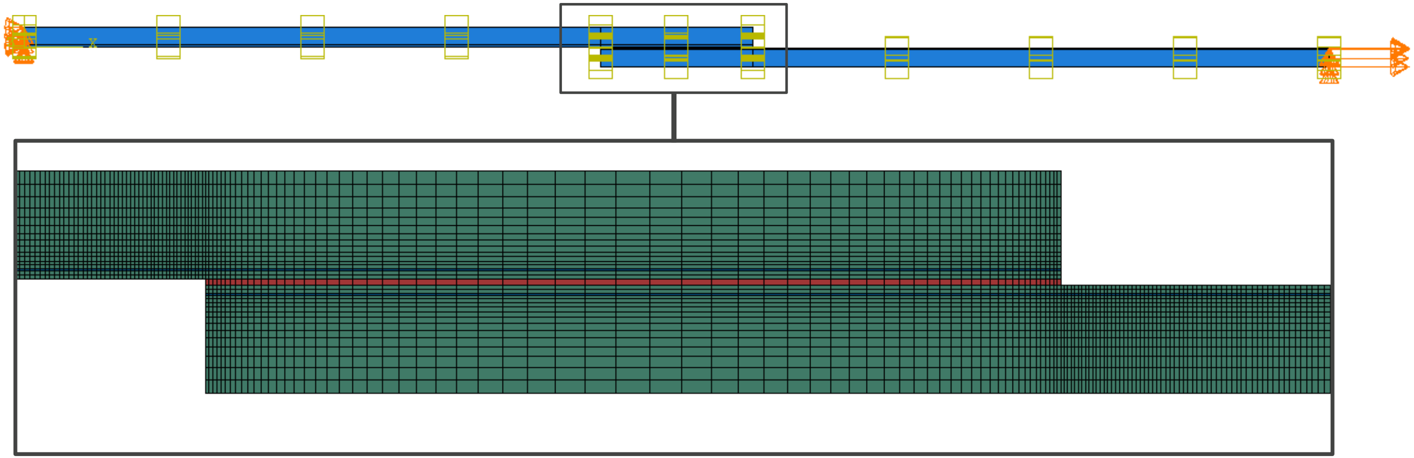

Fig.12 – Boundary conditions and mesh used for the SLJs numerical models.

- **ABAQUS Standard** is used for the quasi-static analysis
- **ABAQUS Explicit** used for the intermediate and impact analysis

Thermal step

- Initial T [°C]: 110
- Final T [°C]: 0

Parameters and methods used for the numerical simulations

CZM models

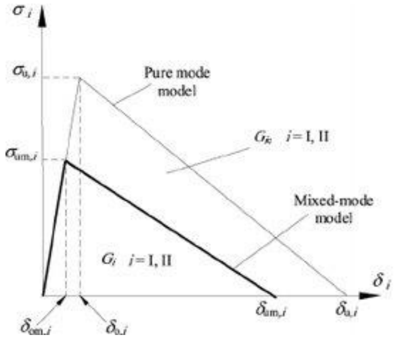

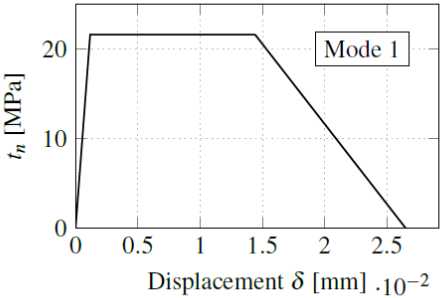

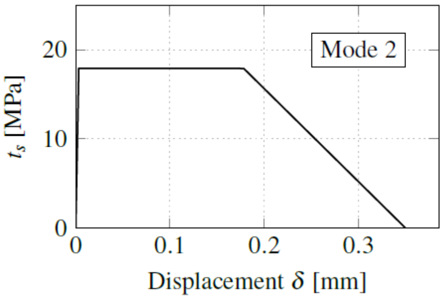

Trapezoidal CZM laws used in the modelling of Araldite®2015-1 for Mode 1 and Mode 2.

Damage initiation: QUADS

$$\left\{\frac{\langle t_n \rangle}{t_n^0}\right\}^2 + \left\{\frac{t_s}{t_s^0}\right\}^2 = 1$$

Mixed mode behaviour: Power law ($\beta = 1$)

$$\left\{\frac{G_n}{G_n^c}\right\}^\beta + \left\{\frac{G_{s1}}{G_s^c}\right\}^\beta = 1$$

Parameters and methods used for the numerical simulations

Influence of the damage initiation criteria in crack propagation

Stress-based criteria are more **sensible to stress concentrations** [Campilho, et al,. 2011], underpredicting the failure load. Hence, strain based criteria are the most suitable ones.

Damage initiation: QUADE

$$f = \left\{\frac{\langle \varepsilon_n \rangle}{\varepsilon_n^0}\right\}^2 + \left\{\frac{\varepsilon_s}{\varepsilon_s^0}\right\}^2$$

Mixed mode behaviour: Power law ($\beta = 1$)

$$\left\{\frac{G_n}{G_n^c}\right\}^\beta + \left\{\frac{G_{s1}}{G_s^c}\right\}^\beta = 1$$

QUAD (quadratic nominal strain)

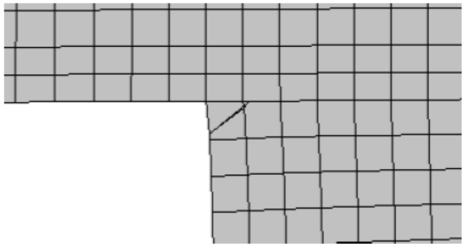

MAXE (maximum nominal strain)

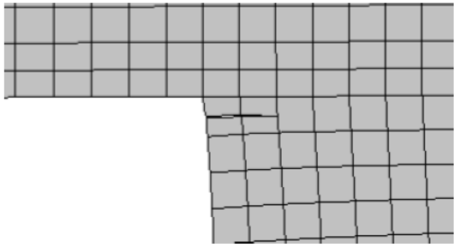

Parameters and methods used for the numerical simulations

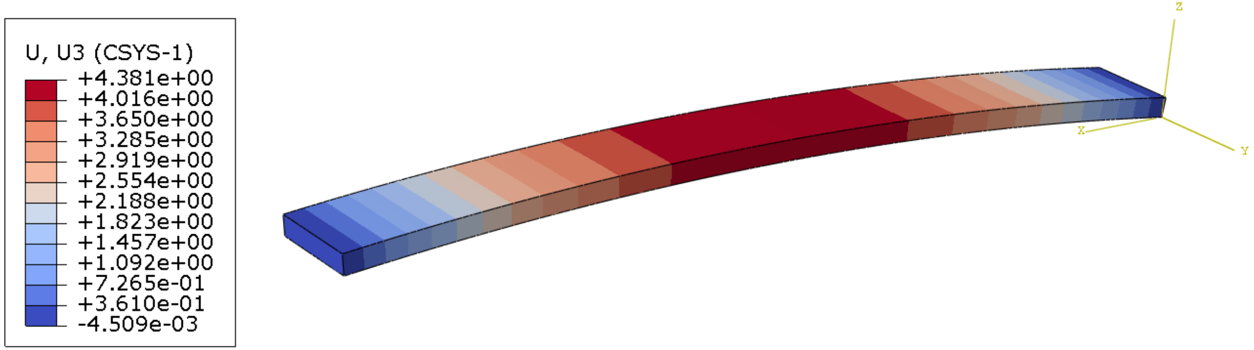

Fig.24 – Numerical simulation results of the composite warpage.

Table 3 – Numerical and experimental results of the observed maximum warpage of the asymmetric composite plates.

Layup	Numerical (mm)	Experimental (mm)	Error (%)
[0°/90°/0°/90°] [LIU et al., 2022]	11.35	11.06	2.6
This study (L5)	3.49	3.51	0.76

Parameters and methods used for the numerical simulations

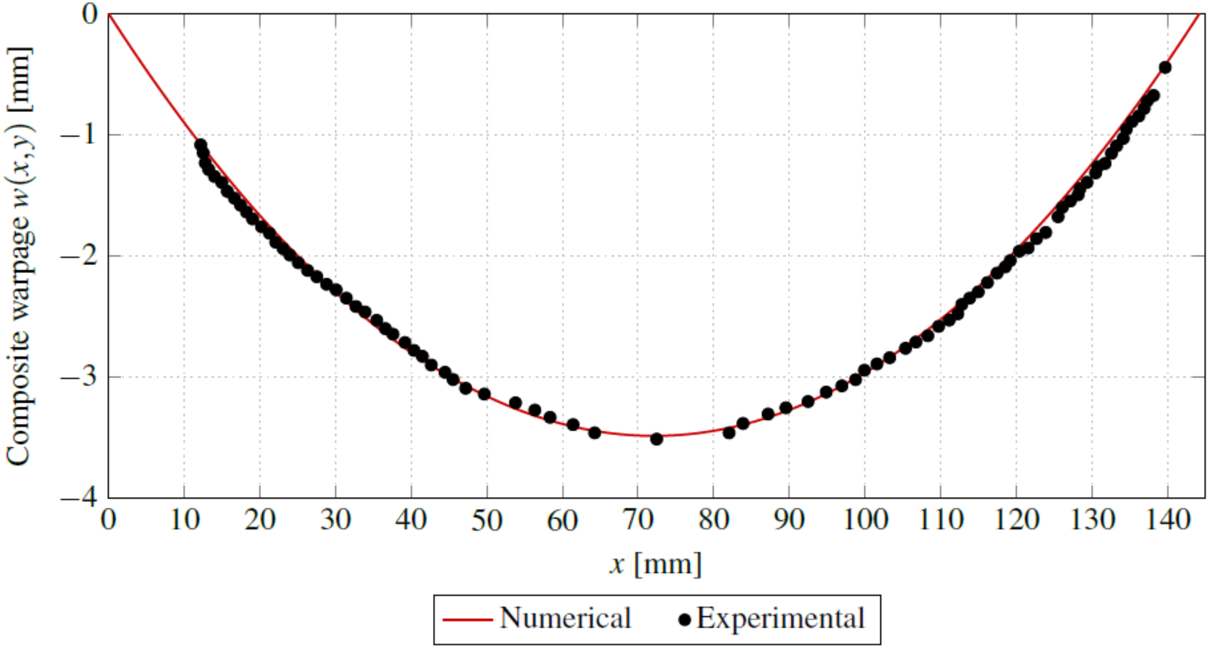

Fig.25 – Warpage of the composite adherend L5 due to thermal stresses.

9.

Backup Slides

Aeronautical application

inegi driving science & innovation

Advanced Joining Processes Unit

Since 1986

U.PORTO

Aeronautical application of the curved SLJ

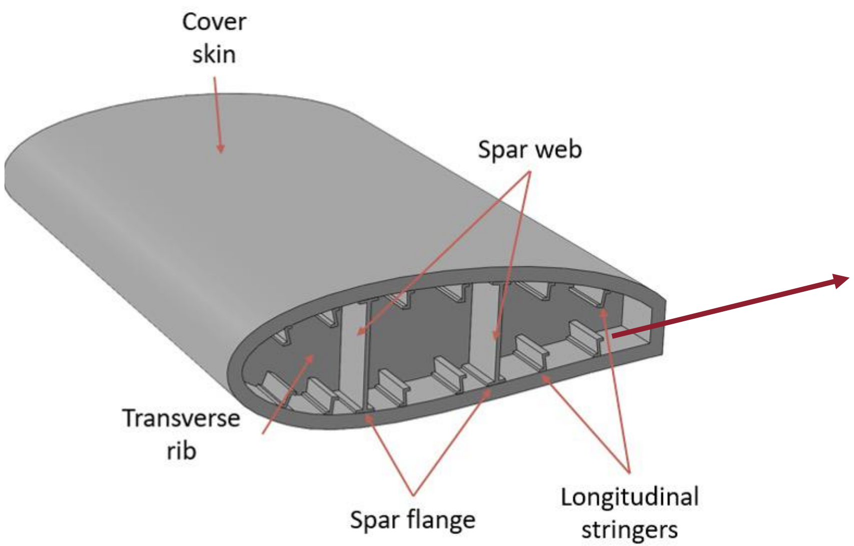

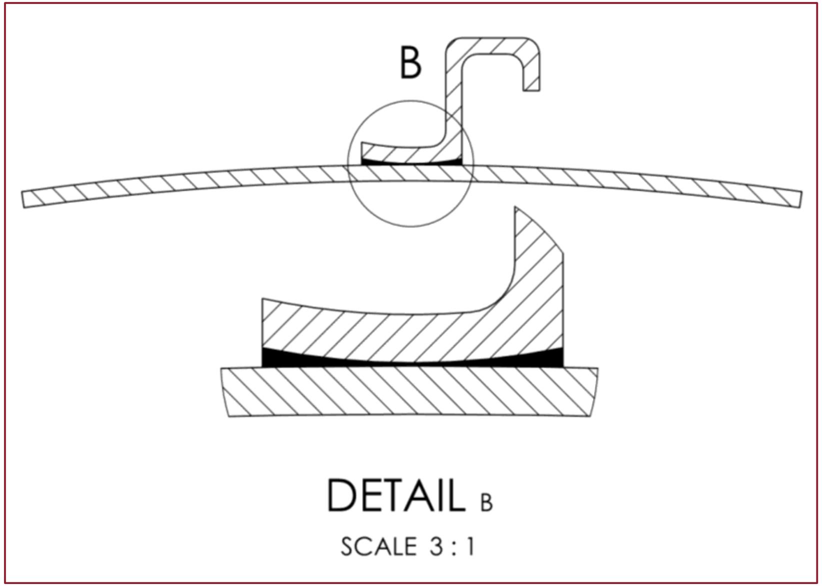

Fig.26 – Example of an aeronautical application of the curved SLJ.

10.

Backup Slides

Other techniques that improve joint strength in composite joints

Since 1986

U.PORTO

Techniques that improve joint strength in composite joints

Surface toughening techniques

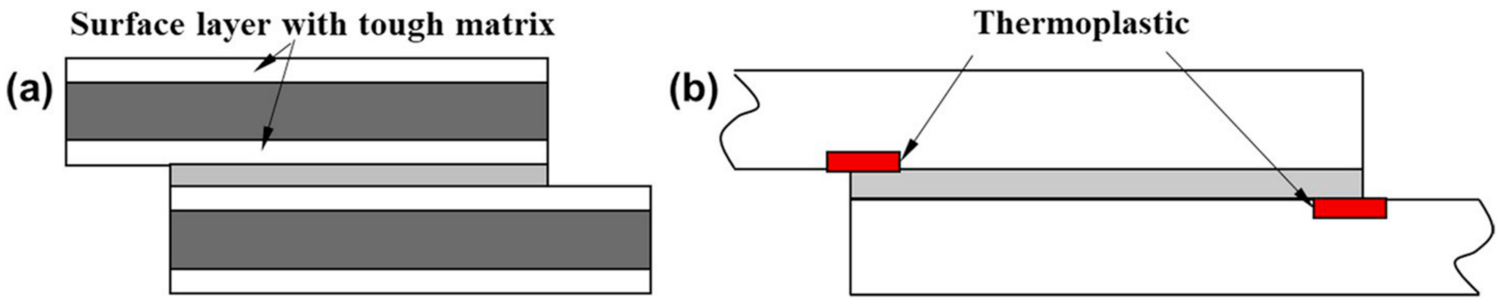

Fig.27 – Schematic of surface toughening techniques [Shang, et al., 2019].

Techniques that improve joint strength in composite joints

Transverse connection

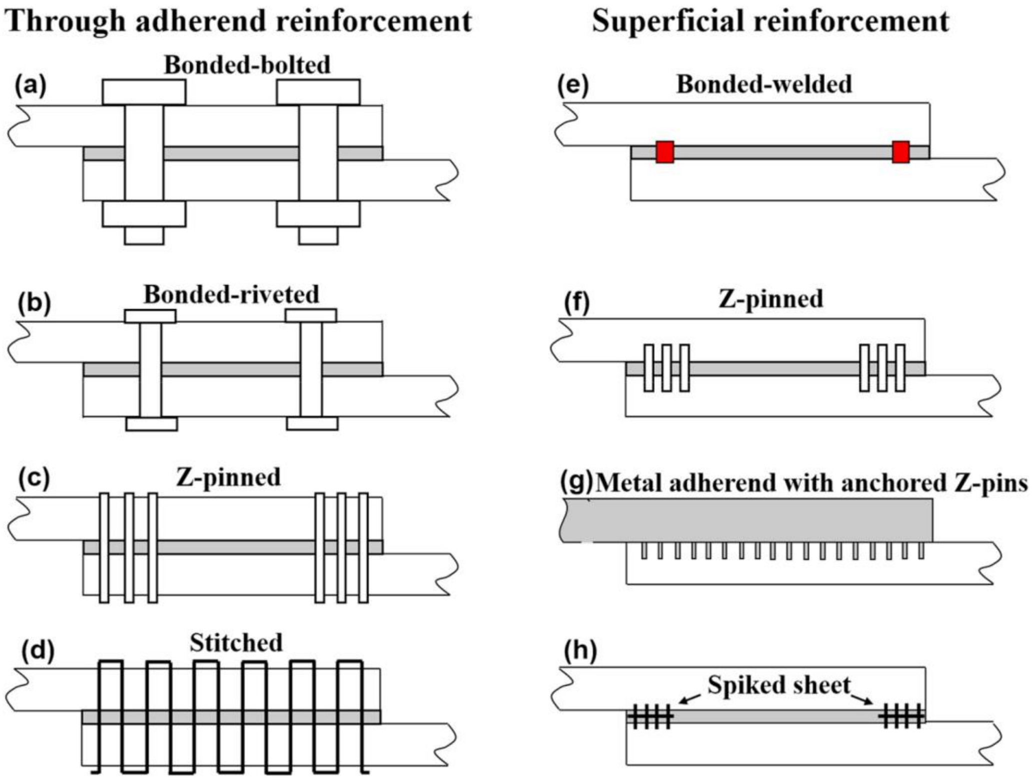

Fig.28 – Schematic representation of transverse connection of adherends [Shang, et al., 2019].